JOURNAL OF GEOPHYSICAL RESEARCH, VOL. 100, NO. C1, PAGES 969–980, JANUARY 15, 1995

Measurements of electromagnetic bias at Ku and C bands

D. V. Arnold,[1,2] W. K. Melville,[3,2] R. H. Stewart,[4] J. A. Kong,[5]
W. C. Keller,[6,7] and E. Lamarre[5]

Abstract. The electromagnetic (EM) bias ε is an error present in radar altimetry of the ocean surface due to nonuniform reflection with surface displacement. The electromagnetic bias is defined as the difference in height between the mean reflecting surface and the mean sea surface. A knowledge of the electromagnetic bias is required for reducing errors in mean sea level measurements by satellite radar altimeters. Direct measurements of the EM bias at 14 GHz (Ku band) and 5 GHz (C band) were made from an oil production platform in the Gulf of Mexico over a 6-month period during 1989 and 1990. A total of 1280 hours of usable data was collected. During the experiment the significant wave height (SWH) varied from 0.6 to 3.2 m; the wind speed at 25 m above the surface varied from 0.1 to 14.3 m s^{-1}; the Ku band bias varied from −1.0 to −13.8 cm, or from −1.6% to −5.3% of the SWH; and the C band bias varied from −0.4 to −19.9 cm, or from −0.6% to −6.3% of the SWH. The biases had mean values of −3.7% and −3.6% of SWH with standard deviations of the variability about the mean of 0.7% and 1.0% of SWH for Ku and C bands, respectively. We found a nonlinear relationship between dimensionless bias (bias/SWH) and wind speed at both low and high wind speeds. For wind speeds less than 3–4 m s^{-1}, both biases were found to be approximately constant. For wind speeds greater than 3–4 m s^{-1} but less than 10 m s^{-1}, both biases were found to increase linearly with wind speed. For wind speeds greater than 11–12 m s^{-1}, the C band bias reaches a maximum. The Ku band bias reaches a maximum and then begins to decrease for wind speeds greater than 9–10 m s^{-1}.

1. Introduction

The electromagnetic (EM) bias ε is an error present in radar altimetry of the ocean surface due to nonuniform reflection of radio signals from wave troughs and crests and is defined as the difference in height between the mean reflecting surface and the mean sea surface. Measurements of electromagnetic bias are needed for reducing errors in mean sea level measurements by satellite radar altimeters.

The electromagnetic bias was first measured by *Yaplee et al.* [1970] from an ocean platform using a 1-ns pulse X band radar. They showed that the reflectivity was not uniform but increased towards the troughs. This caused the mean reflecting surface to be lower than the mean sea surface. The mean reflecting surface was found to be 5% of the significant wave height (SWH) below the mean sea surface.

Satellite radar altimeter measurements (reviewed by *Melville et al.* [1991]) have been used to find upper and lower bounds for the electromagnetic bias. Studies of the GEOS 3, Seasat, and Geosat altimeter data [*Lipa and Barrick*, 1981; *Born et al.*, 1982; *Hayne and Hancock*, 1982; *Douglas and Agreen*, 1983; *Nerem et al.*, 1990] lead to an electromagnetic bias that is in the range of 2–4% of the SWH at Ku band.

During 1980 three airborne electromagnetic bias experiments were performed. *Walsh et al.* [1984] measured the electromagnetic bias at 36 GHz as 1.1% of the SWH. *Choy et al.* [1984] measured the electromagnetic bias at 10 GHz as 3–5% of the SWH. At optical frequencies the electromagnetic bias, measured by *Hoge et al.* [1984], was biased toward the crests by 2% of the SWH for a low wind speed case and biased toward the troughs by 0.75% of the SWH for a high wind speed case. *Walsh et al.* [1989] report additional measurements of the electromagnetic bias at optical frequencies for high wind speed conditions. They found the electromagnetic bias at optical frequencies to be unbiased or biased toward the crests by as much as 0.5% of the SWH.

The work of *Walsh et al.* [1984] and *Choy et al.* [1984] showed a clear dependence of the electromagnetic bias on SWH. It is useful to define a dimensionless bias as

$$\beta = \frac{\varepsilon}{H_{1/3}} \tag{1}$$

where $H_{1/3}$ is the SWH defined as four times the standard deviation of the surface displacement. The measurements of *Choy et al.* [1984] showed a dependence of the dimensionless bias β on the wind speed. During the SAXON-CLT experiment in 1988, *Melville et al.* [1991] measured the electromagnetic bias from an ocean platform at 14 GHz, and they found it was 3.3% of the SWH. A dependence of β on wind speed similar to the result of *Choy et al.* [1984] was found. However, the SAXON-CLT electromagnetic bias experiment contained many more sample points (347 hourly aver-

[1]Brigham Young University, Provo, Utah.
[2]Also at Massachusetts Institute of Technology, Cambridge.
[3]Scripps Institution of Oceanography, La Jolla, California.
[4]Texas A&M University, College Station.
[5]Massachusetts Institute of Technology, Cambridge.
[6]Applied Physics Laboratory, University of Washington, Seattle.
[7]Also at U.S. Naval Research Laboratory, Washington, D. C.

Paper number 94JC02587.
0148-0227/94/94JC-02587$05.00

ages over a 3-week time span) and more accurate wind speed measurements than *Choy et al.* [1984].

During 1989 *Walsh et al.* [1991] measured the electromagnetic bias at 5.3, 13.6, and 36 GHz, and additional measurements were acquired in 1991 at 5.3 and 13.6 GHz [*Hevizi et al.*, 1993]. As in the previous experiments, β was found to depend on the wind speed and the electromagnetic frequency. The airborne electromagnetic bias measurements of *Walsh et al.* [1991] and *Hevizi et al.* [1993] suggest about the same wind speed dependence as the tower measurements of *Melville et al.* [1991], but the airborne measurements of bias are considerably smaller than the tower measurements.

Following our measurements at Ku band [*Melville et al.*, 1991] it became clear that simultaneous bias measurements at both Ku and C band, along with supporting environmental data, were necessary to investigate the frequency dependence of the bias and its relationship to the fine-scale structure of the sea surface. The measurements were necessary to understand the more accurate altimeter data expected from TOPEX/POSEIDON in 1992. A 6-month experiment during winter/spring 1989–1990 was conducted from an oil production platform in the Gulf of Mexico. In this paper we report on the bias measurements at Ku and C bands and their dependence on wind and wave conditions. In a subsequent paper we will describe a semiempirical physical optics scattering theory which uses as input measurements of the high-frequency structure of the sea surface made during the Gulf of Mexico experiment. Preliminary reports of this work have been published by *Melville et al.* [1990] and *Arnold et al.* [1990] (see also *Arnold* [1992]).

2. Description of Experiment and Data Processing

Direct measurements of the electromagnetic bias were made from a Shell offshore oil production platform, the Brazos A-19 complex, in the Gulf of Mexico for a 6-month period from December 1, 1989, to May 31, 1990. The platform complex is located 88 km south-southwest of Freeport, Texas, at 28°10′N and 95°35′W in 40 m of water. The closest land is 58 km to the north-northwest. The platform complex consists of three platforms connected by two bridges forming an L shape (see Figures 1, 2, and 3). Each platform is rectangular in shape with dimensions of 20 m by 50 m in plan. The bridge connecting platforms B and C is 60 m long and the bridge connecting platforms B and D is 50 m long.

2.1. Instrumentation

Nadir-looking, 14-GHz and 5-GHz continuous wave scatterometers, designed and built at the U.S. Naval Research Laboratory, were mounted 18 m above mean sea level at the center of the 60-m bridge connecting platforms B and C. The scatterometers transmit and measure the power reflected from the ocean surface. While the scatterometers do not measure the range to the surface directly, they can infer the wave displacement from the Doppler shift of the scattered signal (see Appendix). The 14-GHz scatterometer antennas had a two-way, 3-dB beam width of 5.0°, corresponding to a 1.6-m diameter footprint. The 5-GHz scatterometer antennas had a two-way, 3-dB beam width of 4.5°, corresponding to a 1.4-m diameter footprint.

A Thorn/EMI infrared wave gauge with a beam width of 1°, corresponding to a 0.3-m diameter footprint, was placed between the two scatterometers where its footprint would lie within the footprints of the scatterometers. The Thorn/EMI infrared wave gauge was operational during the month of February 1990 only. An 8-m capacitance wire wave gauge was suspended from the bridge during intensive experiment periods each of which typically lasted a week. The wire gauge was positioned 15 m away from the scatterometers so as to be outside the scatterometer beams. The wire wave gauge was directly calibrated in situ by raising and lowering the wire by known amounts.

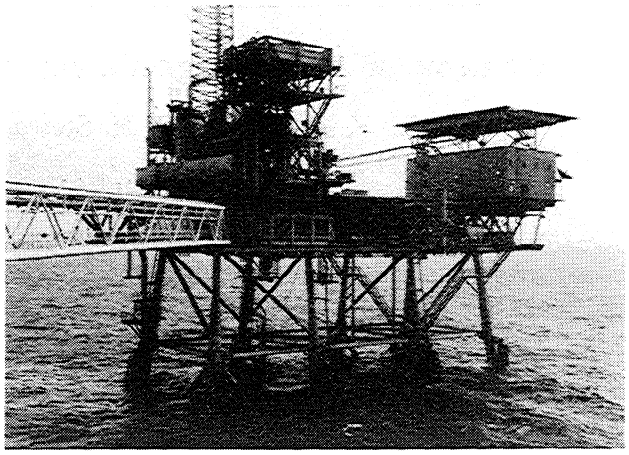

Figure 1. Shell Offshore oil production platform complex Brazos 19, platform C. The scatterometers are mounted at the center of the bridge, in the left foreground.

Wind speed and direction, air temperature, water temperature, rainfall, and relative humidity were measured using an R. M. Young meteorological package. The wind speed, wind direction, and rainfall were measured at the northwest corner of platform B at a height of 25 m above mean sea level. Air temperature and relative humidity were measured at the southwest corner of platform B at a height of 19 m above mean sea level. Water temperature was measured at the south end of platform B at a water depth of 1 m. Unfortunately, the relative humidity and water temperature

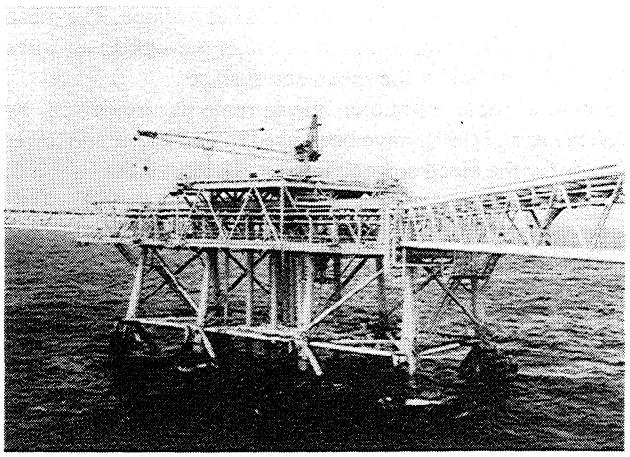

Figure 2. Shell Offshore oil production platform complex Brazos 19, platform B. The scatterometers are mounted at the center of the bridge, in the right foreground.

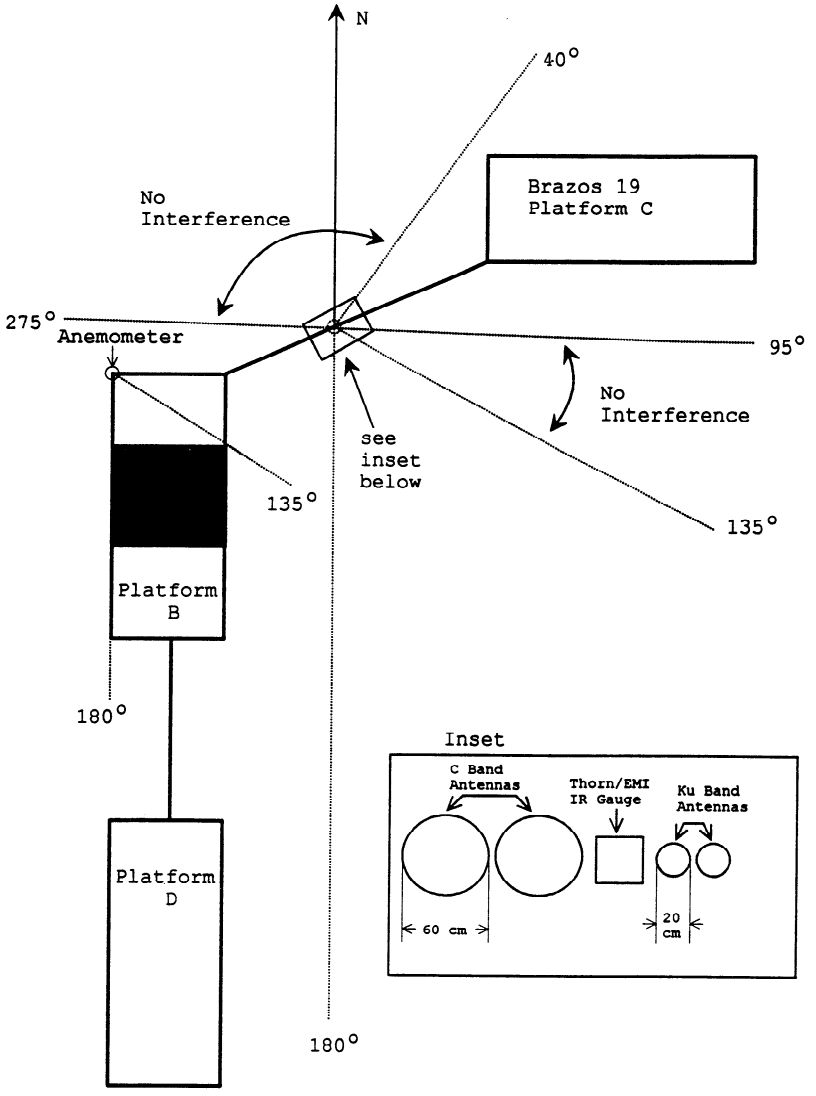

Figure 3. Layout of Brazos 19 platform complex. The platforms are 20 m by 50 m. The bridge between platforms B and C is 60 m long, and the bridge between platforms B and D is 50 m long. The scatterometers were placed in the middle of the bridge between platforms B and C. The layout of the scatterometers is shown in the inset. The platform caused interference with the wave field for directions between 40° and 95° and between 180° and 275°. Structures on platform B caused interference with the wind measurement for directions between 135° and 180°.

measurements were valid for only a small portion of the experiment.

Without the relative humidity and water temperature measurements, it was not possible to accurately translate the wind speed at 25 m to the reference 10-m height. Therefore, wind speed at 25 m will be used in the analysis of the data. Assuming the mean wind velocity profile is logarithmic, and the drag coefficient based on the velocity at 10 m is of the order of 10^{-3}, then winds at 25 m are about 10% larger than winds at 10 m for a neutral atmosphere.

2.2. Data Processing

A digital data acquisition system was used to sample the scatterometer base band signals at 2 KHz; the wind speed, wind direction, and wave gauges at 8 Hz; and the other environmental measurements once every 10 min. The received power and mean Doppler frequency were computed with an integration time of 0.125 s. The mean Doppler frequency was estimated using a time domain covariance processing technique commonly used in weather radar [*Doviak and Zrnic*, 1984]. This technique was also used by *Jessup et al.* [1991] for measuring the Doppler frequency mean and bandwidth for their breaking wave studies (see also *Jessup* [1990]). The data were stored in 10-min. records on optical disks. The mean power and mean Doppler frequency for each scatterometer and the wave gauge signals were stored at an 8-Hz rate. Ten-minute averages of the wind speed, wind direction and the other environmental measurements were stored once every 10 min.

The backscatter power changes with range as r^{-4}, but since the illuminated footprint changes as r^2, the net change in the backscatter power with range is r^{-2}. The backscatter coefficient is given by

$$\sigma^0 = \frac{K(z_0 - \eta)^2}{z_0^2}\,\sigma_m^0 \tag{2}$$

where $z_0 = 18$ m is the height above mean sea level, η is the surface displacement, K is a calibration constant for each scatterometer, and σ_m^0 is the directly measured backscatter power. (It should be noted that there was a typographical error in the first equation in the article by *Melville et al.* [1991, p. 4918]. The equation should read $\sigma_0 = [K(z_0 - \zeta)^2/z_0^2]\sigma_m$.)

The electromagnetic bias was calculated from the measured backscatter coefficient and the measured sea surface displacement using

$$\varepsilon = \frac{\sum_i \sigma_i^0 \eta_i}{\sum_i \sigma_i^0}. \tag{3}$$

Hourly averages of the electromagnetic bias, significant wave height, wind speed, wind direction, and the other environmental measurements were computed from the 10-min. data records.

2.3. Data Editing

The 6 months of data were first edited by hand to remove data for known periods of instrument malfunction. Next, spurious data points with values significantly smaller or larger than expected, which invariably occur in an experiment of this length, were removed by hand.

Next, data contaminated by interference from the platform on the wind and waves were removed. Interference occurred when the waves travelled through the platform structure. The directions corresponding to the platform interference were between 40° and 95° for platform C and between 180° and 275° for platforms B and D (see Figure 3). Also, there was wind blockage by platform B for directions between 135° and 180° (see Figure 3). This left two angular regions, 95° to 135° and 275° to 40°, where the waves and wind were unaffected by the platform structure. Since no measurements of the wave direction were made, the wave direction was assumed to be given by the wind direction for the purpose of removing the platform interference.

3. Results

The Thorn/EMI infrared wave gauge was operational during the month of February 1990, allowing a direct comparison with the measurements from SAXON-CLT in 1988 [*Melville et al.*, 1991]. The data from February will be analyzed first and directly compared with the SAXON-CLT measurements. Next, the data from the entire experiment will be analyzed using wave height calculated from the integrated Doppler centroid measured by the scatterometers. The measurement assumes that the mean Doppler frequency of the nadir-looking scatterometer is proportional to the vertical velocity of the long ocean waves which are longer than the dimensions of the scatterometer footprint. Thus the mean Doppler frequency, when integrated in time, provides an estimate of the sea surface displacement. A calibration of the estimated displacement is obtained by comparing it to the displacement measured with the Thorn/EMI infrared wave gauge during the month of February (see Appendix A).

The preliminary data published by *Melville et al.* [1990] and also appearing in work by *Hevizi et al.* [1993] is different than the results presented here. The preliminary data was taken during February 1990, but the wave height as estimated from the Doppler was not corrected as outlined in Appendix A. The results presented here have been properly corrected.

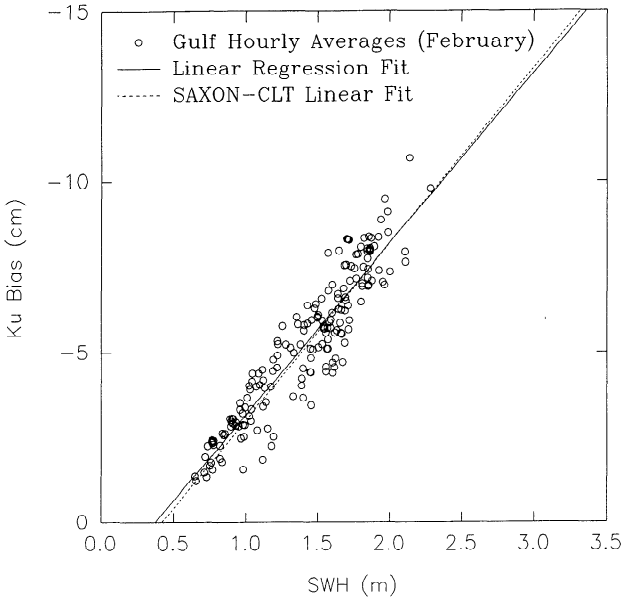

Figure 4. Ku band electromagnetic bias as a function of significant wave height (SWH) for the month of February. The solid line is the linear regression fit ε_{Ku} (cm) = 1.86 − $5.02H_{1/3}$ (m) when $r^2 = 0.859$. The dashed line is the linear regression fit to the data of *Melville et al.* [1991] given by ε_{Ku} (cm) = 2.16 − $5.17H_{1/3}$ (m) when $r^2 = 0.873$.

3.1. Data From the Month of February

A wide range of wind and wave conditions was observed in February 1990. The significant wave height varied from 0.7 to 2.3 m; the wind speed varied from 0.5 to 14.2 m s^{-1}; the Ku band bias varied from −1.2 to −10.7 cm, or from −1.6% to −5.0% of the significant wave height; and the C band bias varied from −1.0 to −12.0 cm, or from −1.4% to −5.7% of the significant wave height. A total of 186 hours of usable data was collected, which resulted in 186 hourly averages.

The February data were used to find the empirical relationships between the electromagnetic bias ε, the significant wave height $H_{1/3}$, and the wind speed U_{25}. The relationships between the bias and the significant wave height for Ku and C bands are shown in Figures 4 and 5, respectively. The linear correlations of the biases and the significant wave height were found to be

$$\varepsilon_{Ku}\ (\text{cm}) = 1.86 - 5.02H_{1/3}\ (\text{m}) \qquad r^2 = 0.86 \tag{4}$$

$$\varepsilon_{C}\ (\text{cm}) = 2.82 - 5.70H_{1/3}\ (\text{m}) \qquad r^2 = 0.80. \tag{5}$$

The correlation of Ku bias and significant wave height, found as part of the SAXON-CLT experiment by *Melville et al.* [1991], was

$$\varepsilon_{Ku}\ (\text{cm}) = 2.16 - 5.17H_{1/3}\ (\text{m}) \qquad r^2 = 0.87. \tag{6}$$

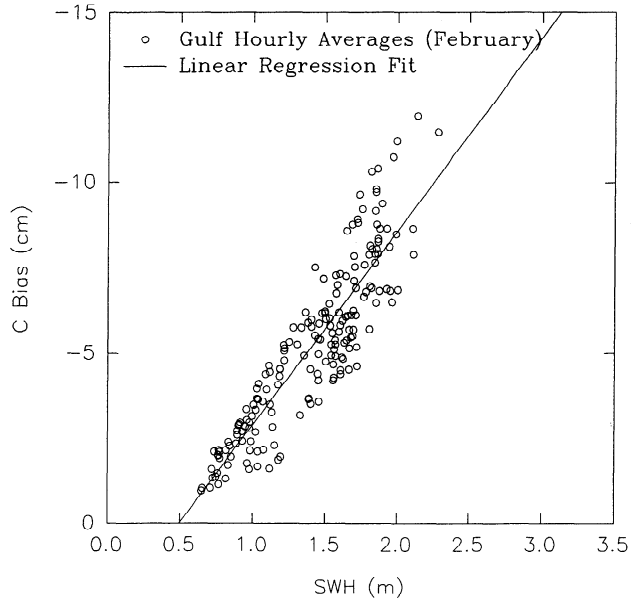

Figure 5. C band electromagnetic bias as a function of significant wave height for the month of February. The solid line is the linear regression fit given by ε_C (cm) = 2.82 − 5.70$H_{1/3}$ (m) when r^2 = 0.797.

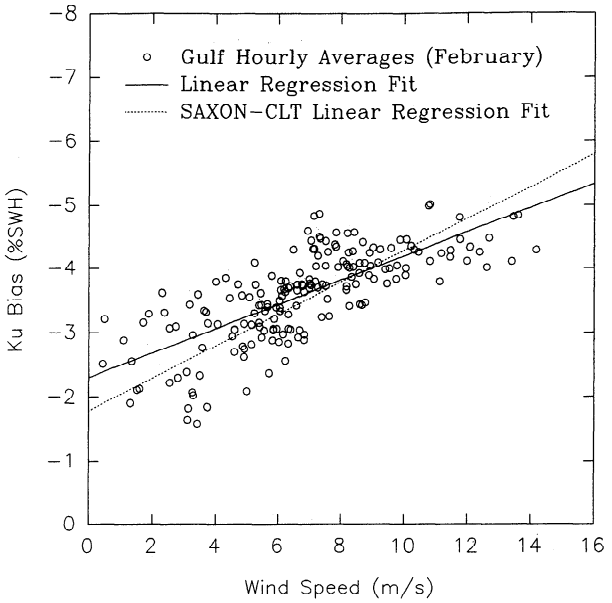

Figure 6. Normalized Ku band electromagnetic bias as a function of wind speed at 25 m above the sea surface for the month of February. The solid line is the linear regression fit β_{Ku} (%SWH) = −2.30 − 0.190U_{25} (m s^{-1}) when r^2 = 0.545. The dashed line is the linear regression fit to the data of *Melville et al.* [1991] given by β_{Ku} (%SWH) = −1.79 − 0.25U_{10} (m s^{-1}) when r^2 = 0.707.

(It should be noted that there was a typographical error in the caption of Figure 5 in the article by *Melville et al.* [1991]. The linear and quadratic fits should be B = 0.0216 − 0.0517$H_{1/3}$ and B = 0.001 − 0.0210$H_{1/3}$ − 0.0104$(H_{1/3})^2$, respectively.) The linear regressions of (4) and (6) are shown as solid and dashed lines, respectively, in Figure 4. Both experiments exhibit essentially the same correlation between the Ku band bias and the significant wave height.

Because of the strong correlation between the bias and the significant wave height, the dimensionless bias $\beta = \varepsilon/H_{1/3}$ is used in the following analysis. The mean value of β_{Ku} was −3.6% with a standard deviation of 0.7%. The mean value of β_C was −3.5% with a standard deviation of 1.0%. For SAXON-CLT [*Melville et al.*, 1991] the mean value of β_{Ku} was −3.5% with a standard deviation of 1%.

The relationships between β and the wind speed for Ku and C bands are shown in Figures 6 and 7, respectively. The linear correlations between β and the wind speed were found to be

$$\beta_{Ku}(\%H_{1/3}) = -2.30 - 0.190U_{25}\ (\text{m s}^{-1}) \quad r^2 = 0.55. \quad (7)$$

$$\beta_C(\%H_{1/3}) = -1.53 - 0.294U_{25}\ (\text{m s}^{-1}) \quad r^2 = 0.69. \quad (8)$$

The correlation of β_{Ku} and the wind speed for SAXON-CLT [*Melville et al.*, 1991] was

$$\beta_{Ku}(\%H_{1/3}) = -1.79 - 0.25U_{10}\ (\text{m s}^{-1}) \quad r^2 = 0.71. \quad (9)$$

The linear regressions of (7) and (9) are shown as solid and dashed lines, respectively, in Figure 6. The difference between these two linear regressions can be attributed to the lower bias at wind speeds greater than 10 m s^{-1} for the present experiment as compared to the SAXON-CLT experiment.

The residual bias, after removing the correlation of β with the wind speed, had a standard deviation of 0.48% and 0.55% of significant wave height for Ku and C bands, respectively. The residual bias for SAXON-CLT, after removing the correlation of β with the wind speed, had a standard deviation of 0.51%.

It should be noted that the correlation coefficient of (7) is much smaller than that for (9). This indicates that the dependence of β on the wind speed is more nonlinear for the

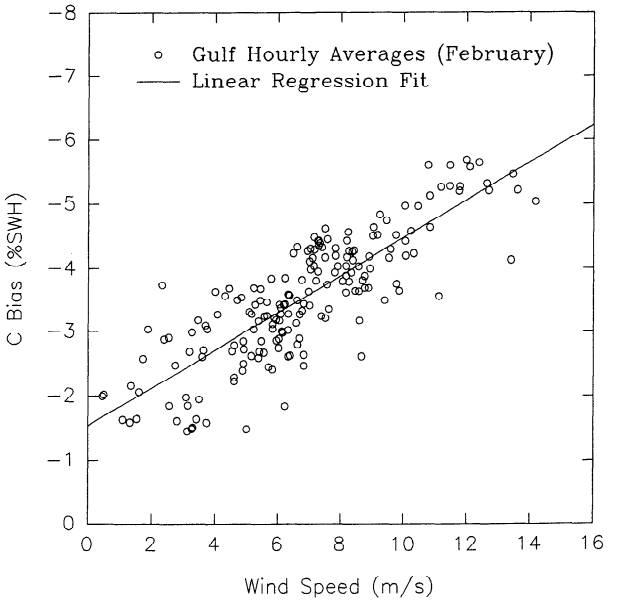

Figure 7. Normalized C band electromagnetic bias as a function of wind speed at 25 m above the sea surface for the month of February. The solid line is the linear regression fit β_C (%SWH) = −1.53 − 0.294U_{25} (m s^{-1}) when r^2 = 0.689.

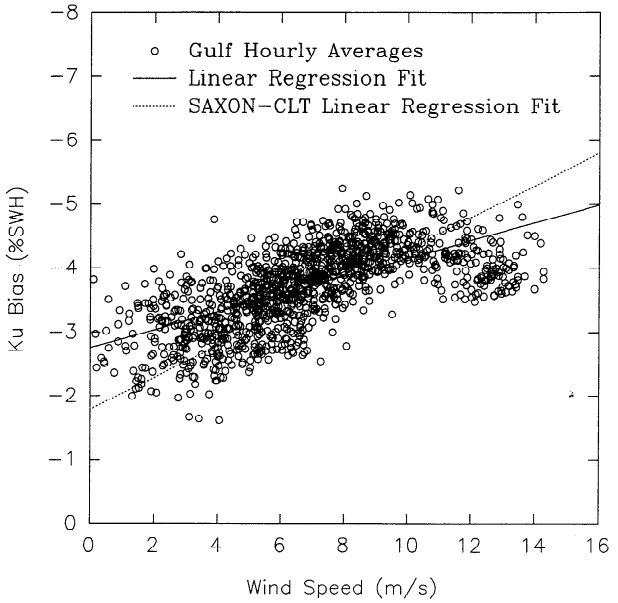

Figure 8. Normalized Ku band electromagnetic bias as a function of wind speed at 25 m above the sea surface for the 6 months of the experiment. The solid line is the linear regression fit β_{Ku} (%SWH) = $-2.76 - 0.139U_{25}$ (m s^{-1}) when $r^2 = 0.417$. The dashed line is the linear regression fit to the data of *Melville et al.* [1991] given by β_{Ku} (%SWH) = $-1.79 - 0.25U_{10}$ (m s^{-1}) when $r^2 = 0.707$.

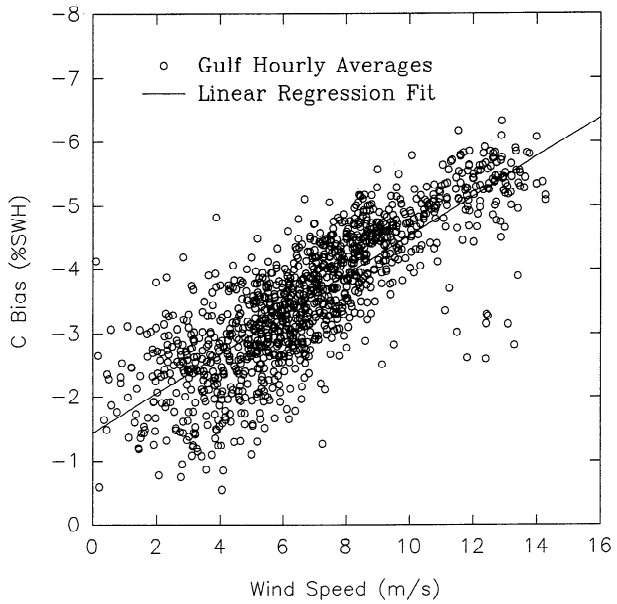

Figure 9. Normalized C band electromagnetic bias as a function of wind speed at 25 m above the sea surface for the 6 months of the experiment. The solid line is the linear regression fit β_C (%SWH) = $-1.44 - 0.309U_{25}$ (m s^{-1}) when $r^2 = 0.661$.

Gulf of Mexico data than for the SAXON-CLT data. Significant nonlinearity can be seen in Figure 6. The nonlinearity will be considered in more detail when discussing the data from the entire 6 months of the experiment.

3.2. Data From Entire 6 Months of the Experiment

The experimental data from the entire 6 months of the experiment will now be analyzed using the bias computed using the integrated scatterometer Doppler centroid for the wave displacement. During the 6 months of the experiment the significant wave height varied from 0.6 to 3.2 m; the wind speed varied from 0.1 to 14.3 m s^{-1}; the Ku band bias varied from -1.0 to -13.8 cm, or from -1.6% to -5.3% of the significant wave height; and the C band bias varied from -0.4 to -19.9 cm, or from -0.6% to -6.3% of the significant wave height. There were a total of 1280 hours of usable data.

The relationships between β and the wind speed for Ku and C bands are shown in Figures 8 and 9, respectively. The linear correlations between β and the wind speed were found to be

$$\beta_{Ku}(\%H_{1/3}) = -2.76 - 0.139U_{25} \qquad r^2 = 0.42. \qquad (10)$$

$$\beta_C(\%H_{1/3}) = -1.44 - 0.309U_{25} \qquad r^2 = 0.66. \qquad (11)$$

The residual bias, after removing the correlation of β with the wind speed, had a standard deviation of 0.48% and 0.65% of significant wave height for Ku and C bands, respectively.

Figure 8 clearly shows a nonlinear dependence of the Ku band dimensionless bias β on the wind speed; less so for C band in Figure 9. To better represent the nonlinear behavior, the bias was binned with wind speed. For each 1-m/s interval in wind speed the bias was averaged. Figure 10 shows the number of hours of data occurring at each 1-m s^{-1} interval of wind speed, and Figure 11 shows the average bias at each 1-m s^{-1} interval. For wind speeds less than 3–4 m s^{-1} the Ku and C band biases are almost constant. Above wind speeds of 3–4 m s^{-1} the biases increase linearly until they reach a maximum. The Ku band bias reaches a maximum at wind speeds of 9–10 m s^{-1}, above which it decreases. The C band bias appears to reach a maximum at wind speeds of 12–14 m s^{-1}, the upper limit of our wind speed measurements.

Figure 12 shows a comparison of the averaged Ku and Cu

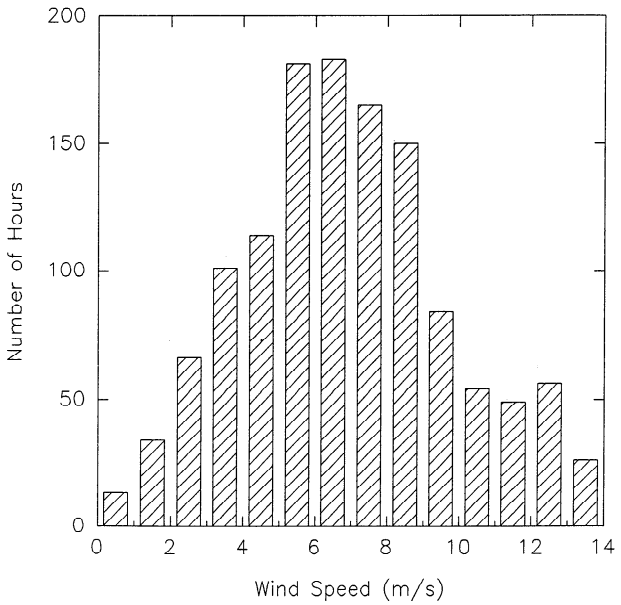

Figure 10. Histogram showing the number of hours of data occurring at each 1 m s^{-1} interval of wind speed for the 6-month experiment.

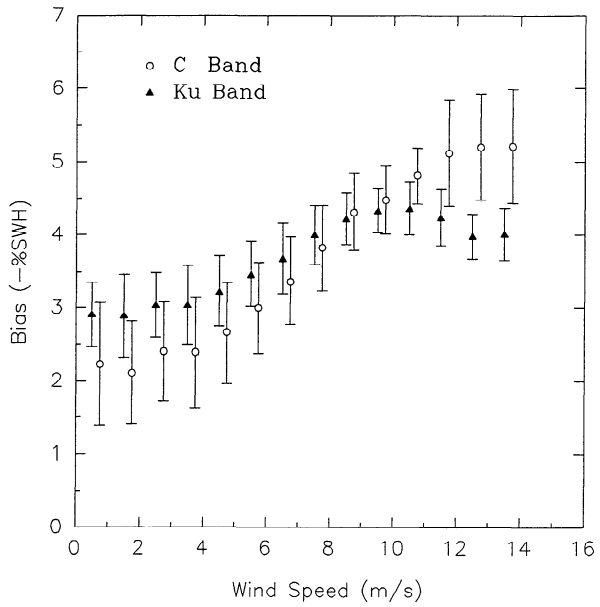

Figure 11. Average normalized electromagnetic bias at each 1 m s^{-1} interval of wind speed as a function of wind speed at a height of 25 m. The vertical bars show the standard deviation about the mean.

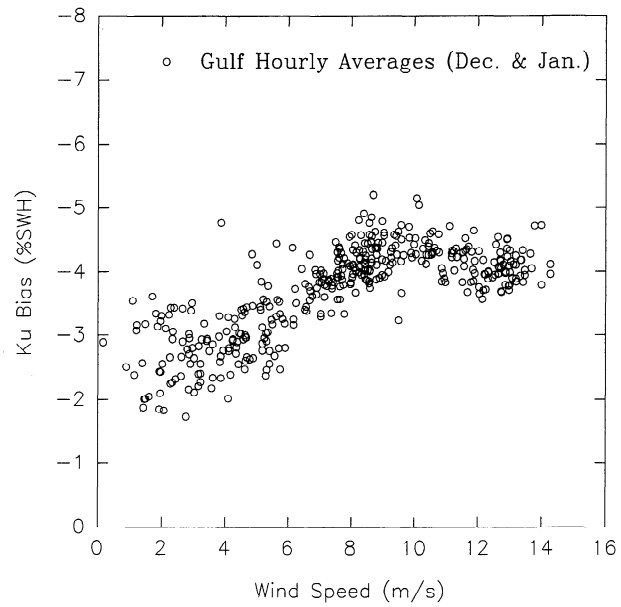

Figure 13. Normalized Ku band electromagnetic bias as a function of wind speed at 25 m above the sea surface for the months of December and January.

band biases from Figure 11. For values of normalized bias less than 4%, the Ku band bias is larger than the C band bias by as much as 0.8% of SWH. For values of normalized bias greater than 4% the C band bias is larger than the Ku band bias by as much as 1% of SWH. Since the bias is a function of wind speed, this result can also be stated in terms of wind speed. For wind speeds less than 10 m s^{-1} the C band bias is less than the Ku band bias. For wind speeds greater than 10 m s^{-1} the C band bias is greater than the Ku band bias.

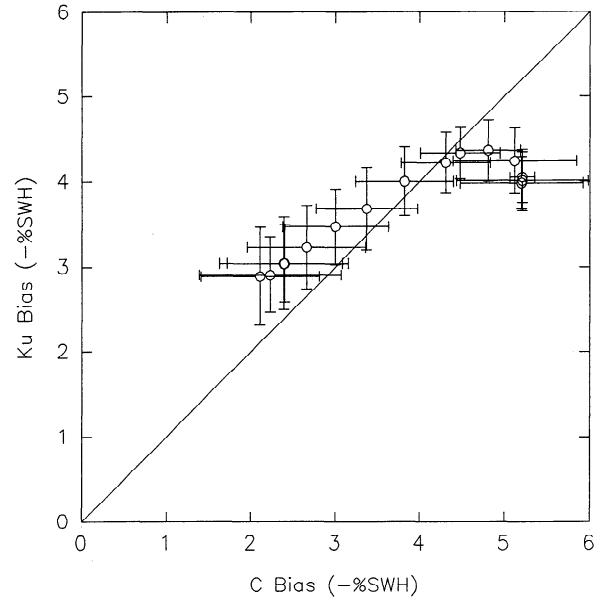

Figure 12. Average normalized Ku band electromagnetic bias compared to the average normalized C band electromagnetic bias. The vertical bars show the standard deviation of the Ku band bias about its mean. The horizontal bars show the standard deviation of the C band bias about its mean.

4. Discussion

The results for the month of February, shown in Figures 6 and 7, compare well with the results for the entire experiment, shown in Figures 8, 9, and 11. The only observable difference between the two is the different behavior of the Ku band bias at wind speeds above 10 m s^{-1}. The Ku band bias, as measured in the month of February (see Figure 6), showed a saturation at wind speeds above 10 m s^{-1}, whereas the Ku band bias measured during the entire experiment (see Figures 8 and 11) shows a decrease in bias above 10 m s^{-1}. Measurements from SAXON-CLT [*Melville et al.*, 1991] showed a saturation at high wind speeds similar to the measurements for the month of February.

A closer examination of the measurements from the months of December and January show a decreasing Ku band bias at wind speeds greater than 10 m s^{-1} (see Figure 13), whereas during February the Ku band bias reached a maximum but did not decrease (see Figure 6). The primary difference between the months of December and January and the month of February was the range of wave heights. During December and January the wave height ranged from 0.6 to 3.2 m, whereas during the month of February the wave height ranged from 0.7 to 2.3 m. The range of wind speed was the same for all three months with wind speed ranging up to 14 m s^{-1}. This explains the differences in the Ku band bias data between February and the entire experiment and indicates a possible dependence of the Ku band dimensionless bias upon the wave height or the wave development at wind speeds above 10 m s^{-1}.

As in previous experiments the dimensionless bias β has been found to depend on the wind speed and the electromagnetic frequency. Figure 14 summarizes the measurements of the present experiment, the SAXON-CLT EM bias measure-

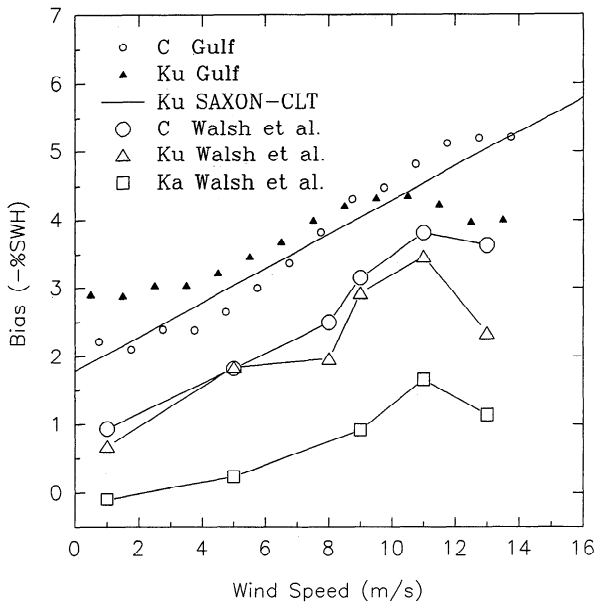

Figure 14. Summary plot showing the normalized electromagnetic bias as a function of wind speed for the present Gulf of Mexico measurements, the SAXON-CLT measurements of *Melville et al.* [1991], and the aircraft measurements of *Walsh et al.* [1991].

ments of *Melville et al.* [1991], and the aircraft EM bias measurements of *Walsh et al.* [1991].

A comparison of the aircraft measurements of *Walsh et al.* [1991] with the present experiment show similar behavior of the bias at high wind speeds. The C band bias as measured by *Walsh et al.* [1991] reached a maximum at wind speeds above 10–11 m s^{-1}, and the Ku band bias decreased at wind speeds above 10–11 m s^{-1}, in agreement with the present experiment.

At low wind speeds two differences between the aircraft and the present measurements are observed. First, the Ku band bias is larger than the C band bias for the present experiment, whereas the two biases were found to be almost equal at low wind speeds by *Walsh et al.* [1991]. However, a close examination of work by *Hevizi et al.* [1993] shows several aircraft measurements where the Ku band bias is significantly larger than the C band bias. Second, the constant bias at wind speeds below 3–4 m s^{-1}, as observed in the present experiment, was also observed during SAXON-CLT [*Melville et al.*, 1991] but not in the aircraft measurements of *Walsh et al.* [1991]. An examination of *Melville et al.*'s [1991] Figure 6 shows a constant bias for wind speeds less than 4 m s^{-1}, with an exception of the 5 hours of data in the wind speed range of 0–1 m s^{-1}.

While the measurements give no direct evidence of the causes of the different bias regimes, it is possible that wave breaking may play a role. For example, at the lower wind speeds a wind speed of 3–4 m s^{-1} is generally taken to be the onset of visible whitecapping [*Thorpe and Humphries*, 1980]. Steep and breaking waves lead to the generation of parasitic capillary waves and other fine-scale structure near the longer wave crests. This suggests that a qualitative change in the fine-scale structure of the surface may begin at 3–4 m s^{-1}. This observation might also be caused by the removal of all wave conditions for which the significant wave height was less than 0.5 m (due to the Doppler wave displacement estimates). At low wind speeds the waves with 0.5 m SWH would be predominantly swell. This might explain the constant bias at low wind speeds.

We know of no strong evidence for a change of regime at wind speeds of 10–12 m s^{-1}. However, wave breaking may also play a role here too. At some higher wind speed we expect small-scale breaking to occur over the whole surface and not just be confined to the crests of the longer waves. As the fine-scale roughness of the surface tends to a homogeneous state relative to wave height, the bias decreases. While this is speculation, these effects could be measured and are perhaps worth further study.

For wind speeds less than 10 m s^{-1}, the Ku band bias as measured in the present experiment was nearly a constant 0.3% of significant wave height larger than the Ku band bias measured in SAXON-CLT, and the bias as measured in SAXON-CLT was nearly a constant 1% of significant wave height larger than the Ku band bias measured by *Walsh et al.* [1991]. This difference may be due to the different heights from the surface at which the measurements were taken. The present experimental measurements, the SAXON-CLT bias measurements, and the aircraft bias measurements were taken at 18, 22, and 160 m above mean sea level, respectively. This could indicate that the closer the measurements are made to the sea surface, the larger the measured bias. *Walsh et al.* [1991] suggested that the height difference may be due to spherical wave front curvature. This idea is analyzed in Appendix B, where it is shown that the spherical wave front curvature is an unlikely explanation of the differences between the tower and aircraft observations. At this time the cause of the constant 1% difference between the tower and aircraft observations is unknown.

Overall, the present experimental measurements compare well with the earlier SAXON-CLT bias measurements

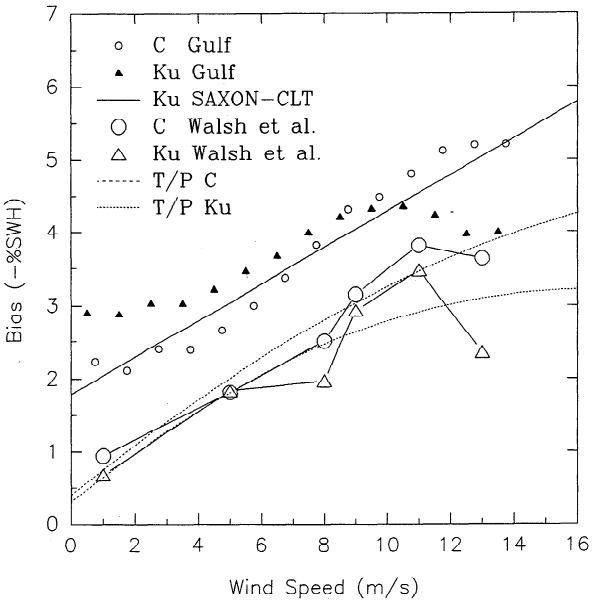

Figure 15. Summary plot comparing the present Gulf of Mexico measurements, the SAXON-CLT measurements of *Melville et al.* [1991], the aircraft measurements of *Walsh et al.* [1991], and the initial TOPEX/POSEIDON EM bias model functions.

[*Melville et al.*, 1991], with the noted exceptions at high wind speeds and the possible measurement height dependence. Also, the tower measurements and the aircraft measurements of *Walsh et al.* [1991] are in good agreement except for the noted constant difference of 1%–1.3% of significant wave height.

The models for correcting the initial data from the TOPEX/POSEIDON mission were [*Hevizi et al.*, 1993]

$$\varepsilon_C(\%\text{SWH}) = -0.40 - 0.358U + 0.0073U^2$$
$$\varepsilon_{Ku}(\%\text{SWH}) = -0.30 - 0.358U + 0.011U^2. \quad (12)$$

Figure 15 compares the initial TOPEX/POSEIDON models given above with the tower and aircraft measurements. The TOPEX/POSEIDON models compare well with the aircraft measurements because they were based on the aircraft measurements. The differences between the tower measurements and the TOPEX/POSEIDON models are the same as the differences between the tower and aircraft measurements discussed above. However, both the aircraft and the tower measurements indicate that the Ku band bias decreases above 10–12 m s^{-1}, and this observation is not fully described by the initial TOPEX/POSEIDON models.

Appendix A. Estimated Wave Displacement From Doppler

Since the Thorn/EMI infrared wave gauge was operational during only one month of the experiment, it was necessary to use the integrated scatterometer Doppler centroid as a measure of the surface wave displacement. Beginning with the assumption that the mean Doppler frequency of the scatterometer (over the 0.125-s sampling interval) is proportional to the vertical velocity of the long ocean waves, the mean Doppler frequency was integrated in time, providing an estimate of the sea surface displacement. Errors in measuring the velocity caused slow time-varying error trends in the estimated wave displacement. The error trends were corrected by computing a 1-min running average of the wave displacement and then removing it. Figure A1 shows comparison of the time series of surface displacement measured with the Thorn/EMI infrared wave gauge and the C and Ku band integrated Doppler. Figure A2 shows a comparison of the significant wave height measured with the Thorn/EMI infrared wave gauge during the month of February as compared to the significant wave height estimated from the scatterometer Doppler. It should be noted that wave heights less than 0.5 m were not used because the wave height estimated from the scatterometer Doppler was grossly in error for small wave heights. Also, since using the Ku band Doppler to estimate the wave displacement was slightly better than using the C band Doppler, the Ku band Doppler was used.

As seen in Figure A2, there is a linear relationship between the SWH measured with the Thorn/EMI infrared wave gauge and the SWH estimated from the Ku band scatterometer Doppler, given by

$$(H_{1/3})_{\text{Thorn}} = 0.1m + (H_{1/3})_{\text{Doppler}}. \quad (13)$$

The SWH estimated from the scatterometer Doppler is a constant 10 cm less than the SWH measured with the Thorn/EMI wave gauge. This difference is due to the integrated scatterometer Doppler underestimating the wave displacement at the wave troughs and crests, where the vertical velocity of the long waves and the corresponding Doppler is near zero.

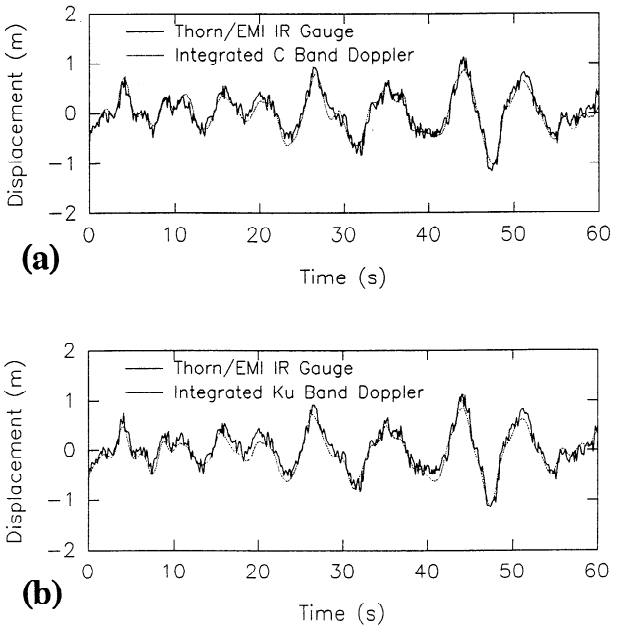

Figure A1. Wave displacement measured using the Thorn/EMI infrared wave gauge compared to the wave displacement measured using the integrated scatterometer Doppler.

The biases computed using the estimated surface displacement from the scatterometer Doppler are compared to the bias computed using the Thorn/EMI wave gauge-measured surface displacement in Figures A3 and A4. As seen in Figures A3 and A4, for Ku band there is no difference

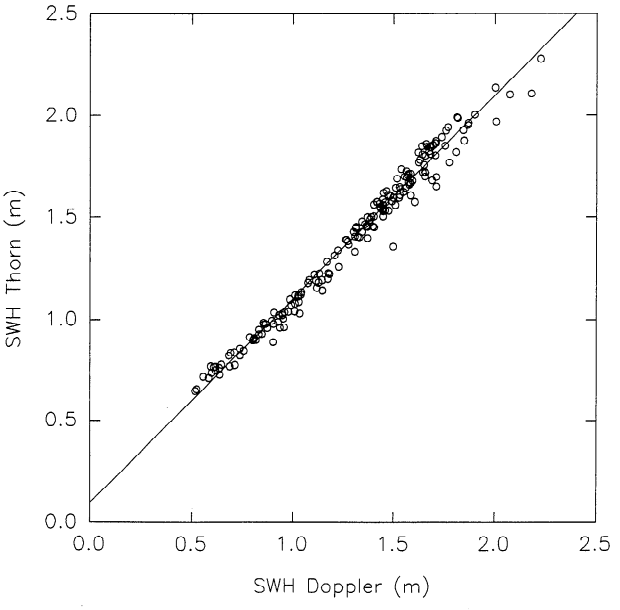

Figure A2. Significant wave height measured using the Thorn/EMI infrared wave gauge compared to the significant wave height measured using the integrated Ku band scatterometer Doppler. The solid line is $(H_{1/3})_{\text{Thorn}} = 0.1$ m + $(H_{1/3})_{\text{Doppler}}$.

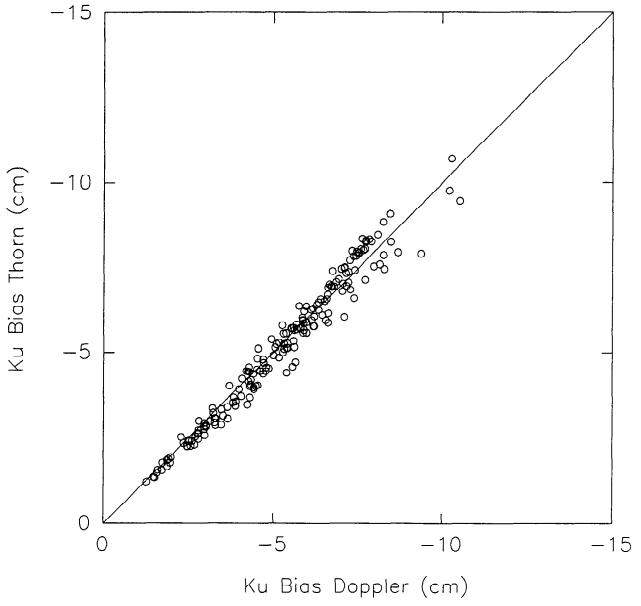

Figure A3. Ku band electromagnetic bias measured using the Thorn/EMI infrared wave gauge compared to the Ku band electromagnetic bias measured using the integrated scatterometer Doppler. The solid line is $(\varepsilon_{Ku})_{Thorn} = (\varepsilon_{Ku})_{Doppler}$.

between the biases computed using the Thorn/EMI wave gauge and those from the scatterometer Doppler, but the C band bias computed using the scatterometer Doppler is a constant 1 cm larger than the bias computed with the Thorn/EMI wave gauge. The reason for this difference is not known. The correspondence between the biases computed using the Thorn/EMI wave gauge and the scatterometer Doppler are given as

$$(\varepsilon_{Ku})_{Thorn} = (\varepsilon_{Ku})_{Doppler} \tag{14}$$

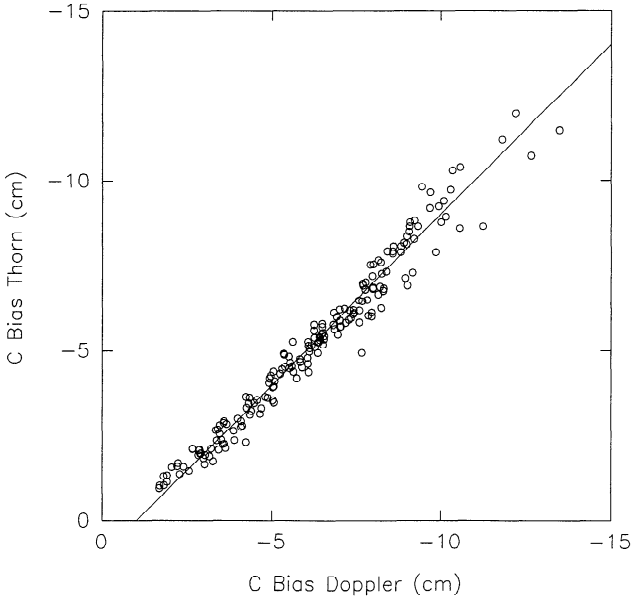

Figure A4. C band electromagnetic bias measured using the Thorn/EMI infrared wave gauge compared to the C band electromagnetic bias measured using the integrated scatterometer Doppler. The solid line is $(\varepsilon_C)_{Thorn} = 1$ cm + $(\varepsilon_C)_{Doppler}$.

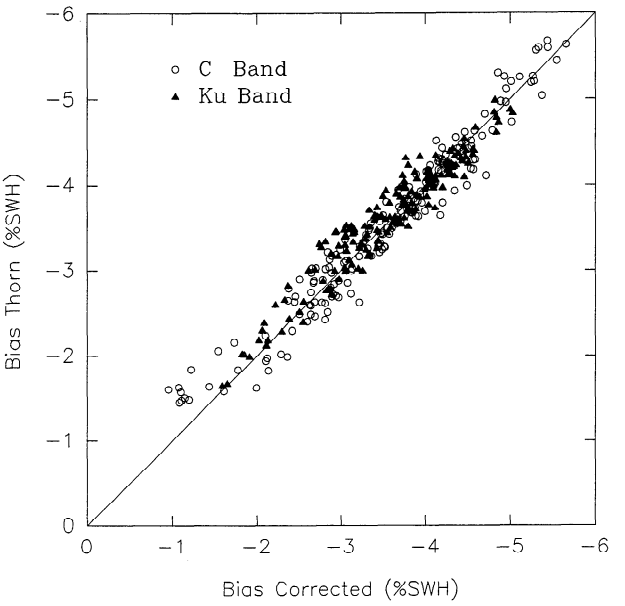

Figure A5. Normalized electromagnetic bias measured using the Thorn/EMI infrared wave gauge compared to the normalized electromagnetic bias measured using the integrated scatterometer Doppler adjusted according to (12), (13), and (14). The standard deviation of the error was 0.233% of SWH for C band and 0.201% of SWH for Ku band.

$$(\varepsilon_C)_{Thorn} = 1 \text{ cm} + (\varepsilon_C)_{Doppler}. \tag{15}$$

Using the Thorn/EMI wave gauge displacement as the standard, the biases and SWH computed using the scatterometer Doppler were adjusted according to (13), (14), and (15). Figure A5 shows the dimensionless bias β, measured using the Thorn/EMI wave gauge, compared to the adjusted dimensionless bias, measured using the scatterometer Doppler. The standard deviation of the error between the adjusted bias and the bias computed using the Thorn/EMI wave gauge was 0.201% of SWH for Ku band and 0.233% of SWH for C band. Figure A5 indicates that the adjusted C band bias underestimates the bias for values less than 1.5% of SWH.

Appendix B. Effect of Wave Front Curvature on EM Bias

Walsh et al. [1991] suggested that the differences between the tower and aircraft experimental results may be due to focusing/defocusing effects of the sea surface structure caused by the spherical electromagnetic wave front. At the sea surface the electromagnetic wave front is spherical, causing an artificial curvature to be added to the sea surface. This has the effect of shifting the effective curvature distribution toward the crests, which could result in a larger electromagnetic bias.

We will analyze this idea and show that it is unlikely that wave front curvature is the cause of the differences between the tower and aircraft experimental results. We will use geometrical optics scattering and a simple unidirectional k^{-3} power law model for the ocean wave spectra. The result will not be exact, but it will give an estimate of the error in the measured bias due to the spherical wave front.

Under the geometrical optics approximation, the back-

scatter power from a specular point on a surface is inversely proportional to the surface curvature at that point. The spherical wave front will add an apparent curvature to the surface. The first task is to find the curvature of a specular point.

The surface will be modeled as unidirectional with a power law spectrum given by

$$S(k) = 2\sigma^2 k_0^2 k^{-3} u(k - k_0) \tag{16}$$

where σ is the surface height standard deviation and k_0 is the lower wavenumber cutoff. When using geometrical optics the surface must be low-pass filtered or else the curvature will be incorrectly dominated by the high-frequency structure of the surface. If the surface is low-pass filtered at the wavenumber k_1, the curvature standard deviation (under the assumption that k_1 is much greater than k_0) is

$$\sigma_c = \sigma k_0 k_1 \qquad k_1 \gg k_0 \tag{17}$$

The surface height standard deviation for waves with wavenumber on the order of k_1 is

$$\sigma_1 = \sigma k_0 / k_1 \tag{18}$$

As seen in (17) the curvature is dominated by the waves with the highest wavenumber. This means that the bias cannot be in error by more than the amplitude of the waves with the highest wavenumber that effect the scattering. Modeling the highest wavenumber wave by a sinusoid with amplitude $2\sigma_1$ and with curvature $-\sigma_C$ at the wave crests and $+\sigma_C$ at the wave troughs, the bias can be computed (the spherical wave front modifies the surface curvature by $1/R$) as

$$\varepsilon = \frac{\Sigma(\eta_i P_i)}{\Sigma(P_i)} = \frac{2\sigma_1\left(\dfrac{1}{\sigma_c + 1/R}\right) - 2\sigma_1\left(\dfrac{1}{\sigma_c - 1/R}\right)}{\dfrac{1}{\sigma_c + 1/R} + \dfrac{1}{\sigma_c - 1/R}}$$

$$= -\frac{2\sigma_1}{\sigma_c R} \tag{19}$$

Substituting (17) and (18) into (19) gives

$$\varepsilon = -\frac{2}{k_1^2 R} \tag{20}$$

Now we must select the high wavenumber cutoff. A lower bound can be found by choosing a wave whose amplitude is at least one half of an electromagnetic wavelength. At Ku and C band the wavelength is between 2.5 and 6 cm, which implies a high wavenumber cutoff for waves with amplitudes less than about 1–3 cm. Waves with length of 1 m have amplitudes on the order of 1 cm, which is chosen as a lower bound for the high wavenumber cutoff. Another way of choosing the high wavenumber cutoff would be to follow *Barrick and Lipa* [1985] and chose a high wavenumber cutoff equal to one tenth of the electromagnetic wavenumber. At C band the electromagnetic wavenumber is 105, giving a high wavenumber cutoff of 10.5, which corresponds to a wavelength of 0.6 m.

Using a 1-m length for the wavenumber cutoff and a range of 18 m from the surface, the error in the bias, computed using (20), becomes 0.28 cm. This is much smaller than the differences observed between the tower and aircraft observations. Also as the wind speed increases the high wavenumber cutoff will increase (the smaller waves will grow in amplitude), which according to (20) will cause the error in the bias to quickly decrease because of the inverse square dependence on the high wavenumber cutoff. This does not match the observed differences between the tower and aircraft observations. The bias as measured on the tower was a constant 1% of SWH height larger than the bias measured from the aircraft for all wind speeds, as seen in Figure 14.

Acknowledgments. We are grateful to Shell Offshore and the crew of the Brazos Platform Complex for access to the facility, logistical support, and hospitality. We thank Francis Felizardo for data gathering. This research was supported by NASA with grants to JAK, RHS, and WKM.

References

Arnold, D. V., Electromagnetic bias in radar altimetry at microwave frequencies, Ph.D. thesis, 180 pp., Dep. of Electr. Eng. and Comput. Sci., Mass. Inst. of Technol., Cambridge, 1992.

Arnold, D. V., W. K. Melville, and J. A. Kong, Theoretical prediction of EM bias, paper presented at Oceans '90, Engineering in the Ocean Environment, Oceanic Eng. Soc. Inst. Electr. Electron. Eng., Washington, D. C., Sept. 24–26, 1990.

Barrick, D. E., and B. J. Lipa, Analysis and interpretation of altimeter sea echo, *Adv. Geophys.*, *27*, 61–100, 1985.

Born, G. H., M. A. Richards, and G. W. Rosborough, An empirical determination of the effects of sea state bias on SEASAT altimetry, *J. Geophys. Res.*, *87*, 3221–3226, 1982.

Choy, L. W., D. L. Hammond, and E. A. Uliana, Electromagnetic bias of 10 GHz radar altimeter measurements of MSL, *Mar. Geod.*, *8*(1–4), 297–312, 1984.

Douglas, B. C., and R. W. Agreen, The sea state correction for GEOS 3 and SEASAT satellite altimeter data, *J. Geophys. Res.*, *88*, 1655–1661, 1983.

Doviak, R. J., and D. S. Zrnic, Meteorological radar signal processing, in *Doppler Radar and Weather Observations*, pp. 91–120, Academic, San Diego, Calif., 1984.

Hayne, G. S., and D. W. Hancock III, Sea-state-related altitude errors in the SEASAT radar altimeter, *J. Geophys. Res.*, *87*, 3227–3231, 1982.

Hevizi, L. G., E. J. Walsh, R. E. MacIntosh, D. Vandemark, D. E. Hines, R. N. Swift, and J. F. Scott, Electromagnetic bias in sea surface range measurements at frequencies of the TOPEX/POSEIDON satellite, *IEEE Trans. Geosci. Remote Sens.*, *31*, 376–388, 1993.

Hoge, F. E., W. B. Krabill, and R. N. Swift, The reflection of airborne UV laser pulses from the ocean, *Mar. Geod.*, *8*(1–4), 313–344, 1984.

Jessup, A. T., Detection and characterization of deep water wave breaking using moderate incidence angle microwave backscatter from the sea surface, Ph.D. thesis, 344 pp., MIT/WHOI Joint Program in Oceanogr. and Oceanogr. Eng., Mass. Inst. of Technol./Woods Hole Oceanogr. Inst., Woods Hole, Mass., 1990.

Jessup, A. T., W. K. Melville, and W. C. Keller, Breaking waves affecting microwave backscatter, *J. Geophys. Res.*, *96*, 20,547–20,569, 1991.

Lipa, B. J., and D. E. Barrick, Ocean surface height-slope probability density function from SEASAT altimeter echo, *J. Geophys. Res.*, *86*, 10,921–10,930, 1981.

Melville, W. K., D. V. Arnold, R. H. Stewart, W. C. Keller, J. A. Kong, A. T. Jessup, and E. Lamarre, Measurements of EM bias at Ku and C bands, paper presented at Oceans '90, Engineering in the Ocean Environment, Oceanic Eng. Soc. Inst. Electr. Electron. Eng., Washington, D. C., Sept. 24–26, 1990.

Melville, W. K., R. H. Stewart, W. C. Keller, J. A. Kong, D. V. Arnold, A. T. Jessup, M. R. Loewen, and A. M. Slinn, Measure-

ments of electromagnetic bias in radar altimetry, *J. Geophys. Res.*, *96*, 4915–4924, 1991.

Nerem, R. S., B. D. Tapley, and C. K. Shum, Determination of the ocean circulation using GEOSAT altimetry, *J. Geophys. Res.*, *95*, 3163–3179, 1990.

Thorpe, S. A., and P. N. Humphries, Bubbles and breaking waves, *Nature*, *283*, 463–465, 1980.

Walsh, E. J., D. W. Hancock, D. E. Hines, and J. E. Kenney, Electromagnetic bias of 36 GHz radar altimeter measurements of MSL, *Mar. Geod.*, *8*, 265–296, 1984.

Walsh, E. J., F. C. Jackson, E. A. Uliana, and R. N. Swift, Observations on electromagnetic bias in radar altimeter sea surface measurements, *J. Geophys. Res.*, *94*, 14,575–14,584, 1989.

Walsh, E. J., et al., Frequency dependence of electromagnetic bias in radar altimeter sea surface range measurements, *J. Geophys. Res.*, *96*, 20,571–20,583, 1991.

Yaplee, B. S., A. Shapiro, D. L. Hammond, B. D. Au, and E. A. Uliana, Nanosecond radar observations of the ocean surface from a stable platform, *IEEE Trans. Geosci. Electron.*, *9*, 170–174, 1971.

D. V. Arnold, Dept. of Electrical and Computer Engineering, Brigham Young University, 459 Clyde Building, Provo, UT 84602. (e-mail: arnold@ecendept.ee.byu.edu)

W. C. Keller, Applied Physics Laboratory, University of Washington, 1013 N.E. 40th St., Seattle, WA 98195.

J. A. Kong and E. Lamarre, Massachusetts Institute of Technology, 26-305, 77 Massachusetts Ave., Cambridge, MA 02139.

W. K. Melville, Scripps Institution of Oceanography, University of California, La Jolla, CA 92093-0213.

R. H. Stewart, Dept. of Oceanography, Texas A&M University, College Station, TX 77843.

(Received October 18, 1993; revised September 29, 1994; accepted September 29, 1994.)